Chapter 2

The Structure of *E. coli* BtuF

and Binding to Its Cognate ABC Transporter, BtuCD

reprinted from PNAS

The structure of *E. coli* BtuF and binding to its cognate ABC transporter

Elizabeth L. Borths, Kaspar P. Locher, Allen T. Lee, Douglas C. Rees*

Howard Hughes Medical Institute and Division of Chemistry and Chemical Engineering, Mail Code 114-96, California Institute of Technology, Pasadena, California 91125, USA

Abstract

Bacterial binding protein-dependent ABC transporters facilitate uptake of essential nutrients. The crystal structure of *E. coli* BtuF, the protein that binds vitamin B_{12} and delivers it to the periplasmic surface of the ABC transporter BtuCD, reveals a bi-lobed fold resembling that of the ferrichrome binding protein FhuD. B_{12} is bound in the "base-on" conformation in a deep cleft formed at the interface between the two lobes of BtuF. A stable complex between BtuF and BtuCD (with the formula $BtuC_2D_2F$) is demonstrated to form *in vitro* and was modeled using the individual crystal structures. Two surface glutamates from BtuF may interact with arginine residues on the periplasmic surface of the BtuCD transporter. These glutamate and arginine residues are conserved among binding proteins and ABC transporters mediating iron and B_{12} uptake, suggesting that they may have a role in docking and the transmission of conformational changes.

Introduction

ABC transporters are a ubiquitous family of importer and exporter proteins that invariably consist of two membrane-spanning domains, that form a translocation pathway, and two cytoplasmic ABC (*A*TP *B*inding *C*assette) domains, that power the transport reaction through binding and hydrolysis of ATP (1). While most eukaryotic ABC transporters export hydrophobic molecules from the cytoplasm (2), the majority of bacterial ABC transporters import essential nutrients that are delivered to them by specific binding proteins (1, 3, 4). These proteins bind their substrates selectively and with high affinity, which is thought to ensure the specificity of the transport reaction (3). The association of a substrate-loaded binding protein with its cognate transporter has been shown to stimulate ATP hydrolysis by the cytoplasmic ABC domains (5). The binding protein remains docked to the cognate transporter until one or both of the hydrolysis products are released, as shown by experiments that used vanadate to trap an intermediate close to the transition state (6). This suggested that the binding protein, associated with the transporter during substrate translocation, may prevent the escape of substrate into the periplasmic space.

The structures of many different binding proteins have been solved, revealing a common architecture: two domains, each consisting of a central β-sheet and surrounding α-helices, with the substrate binding site located in a cleft between them (7). Recently, the crystal structure of the binding protein-dependent ABC transporter, BtuCD, which facilitates import of vitamin B_{12} into *Escherichia coli*, was determined at 3.2 Å resolution

(8). We have now solved the crystal structure of *E. coli* BtuF, the cognate periplasmic binding protein for BtuCD (9, 10) at 2.0Å resolution. In addition, we could form a stable complex between BtuF and BtuCD *in vitro*. These results provide general insights into the interaction of binding proteins with their cognate ABC transporters.

Materials and Methods

Purification and Crystallization. The *btuf* gene (previously *yadt*) was amplified from *Escherichia coli* genomic DNA. A construct with the OmpA signal sequence and an N-terminal Strep-tag II preceding the coding sequence of the mature form of BtuF was subcloned into pET22b (Novagen). The protein was expressed in BL21 DE3 cells (Novagen) grown at 30 ºC in Terrific Broth supplemented with 100 μg/ml ampicillin. The periplasmic extract from approximately 4 g of BtuF expressing cells was concentrated to 4 mL using Centriprep 10 concentrator units. The sample was dialyzed overnight against 2 L of 10 mM Tris, pH = 7.5, 25 mM NaCl at room temperature and subsequently centrifuged to remove precipitated protein. The supernatant was applied to a 1 ml DEAE sepherose column equilibrated in dialysis buffer and the flow through, containing 90-95% pure BtuF, was collected. Although present in the final construct, the Strep-tag II was not used for purificaton. Vitamin B_{12} (cyanocobalamin, Sigma) was added to a final concentration of ~1 mM and the sample was concentrated to 15-20 mg mL^{-1}. The ABC transporter BtuCD was expressed and purified as described (8).

BtuF with bound vitamin B_{12} was crystallized at 4 ºC by vapor diffusion in hanging drops containing 2 μL protein and 2 μL reservoir solution (30% PEG 400, 0.1 M sodium acetate, pH=4.6, 0.1 M cadmium chloride, Hampton Crystal Screen 2, #12). Ruby-red hexagonal bipyramidal crystals appeared within 3 days. Crystals were transferred to a 20 μL drop of reservoir solution containing ~5 mM vitamin B_{12}, incubated for 5-15 minutes, and frozen in liquid nitrogen. The crystals were in the space group $P6_5$ (a = b = 133.07 Å, c = 67.69 Å) with two molecules per asymmetric unit.

Data collection and structure determination. Data was collected from a single crystal at the Stanford Synchrotron Radiation Laboratory beam line 9-2 at 100 K with an ADSC Quantum-315 CCD detector and processed using DENZO and SCALEPACK (11). Experimental phases were obtained from a three wavelength MAD experiment at the cobalt edge. The cobalt sites were found using SOLVE (12) and their parameters refined with SHARP (13). Solvent flattening, two-fold non-crystallographic symmetry (NCS) averaging and phase extension to 2.0 Å were performed with DM (14) and the resulting maps, calculated using FFT (14), were of excellent quality. Anomalous difference Fourier maps were used to visualize the B_{12}-bound cobalts as well as ordered cadmium and chlorine ions bound to the surface of the protein. Cadmium versus chlorine ions were distinguished by the intensities of the anomalous difference Fourier peaks. Peaks in the anomalous difference Fourier map were also observed at positions corresponding to sulfur atoms in cysteine and methionine residues, and to the phosphorus atom in each B_{12} molecule. The protein model was built using O (15) and was refined against data combined from all wavelengths using CNS (16). NCS restraints were released after

initial rounds of refinement and each molecule was refined separately. Model quality was verified using PROCHECK (17). The final model contains two molecules of BtuF including residues 23 to 266 (the entire mature protein) plus one residue at the N-terminus from the Strep-tag II linker (Ala22). 377 waters, 22 cadmium and 6 chlorine ions and 1 PEG400 molecule complete the model. The coordinates have been deposited in the Protein Data Bank (PDB code: 1N2Z) for release upon publication. Figures 1, 2 and 4*A* were prepared using DINO (18).

Results and Discussion

Structure of BtuF and the Vitamin B_{12} binding site. The crystal structure of *E. coli* BtuF with bound vitamin B_{12} was solved using phases obtained from a MAD experiment at the cobalt edge. Data collection, phasing and refinement statistics are presented in Table 1. BtuF has two structurally similar domains (lobes), each consisting of a central five-stranded β-sheet surrounded by helices (Rossmann-like fold). The domains are connected by a single "backbone" α-helix spanning the length of the protein (Fig. 1). This pattern of inter-domain connectivity has also been observed in the Mn^{2+}-binding protein PsaA from *Streptococcus pneumoniae* (19), the Zn^{2+}-binding protein TroA from *Treponema pallidum* (20), and the ferrichrome-binding protein FhuD from *Escherichia coli* (21). None of these binding proteins fall into the previously defined Group I or Group II, characterized by three or two inter-domain connections respectively (7), but instead form a third Group, characterized by a single α−helical segment bridging the two lobes.

Data collection

	peak	inflection	remote
Wavelength (Å)	1.60268	1.60518	1.03317
Resolution (Å)	20-2.0Å	20-2.0Å	20-2.0Å
Unique reflections	46209	46201	46346
Redundancy	19.5	19.5	10.1
Completeness[1]	99.9 (98.7)	99.9 (98.5)	100 (100)
$I/\sigma(I)$[1]	35.8 (7.7)	35.8 (7.4)	34.6 (11.1)
Rsym[1]	9.3 (28.8)	9.0 (29.0)	5.8 (18.2)

Phasing from Co MAD dataset

Resolution	20-2.5Å
Isomorphous phasing power from peak (centric/acentric)	7.61/11.93
Anomalous phasing power from peak (acentric)	2.22
Isomorphous phasing power from inflection (centric/acentric)	7.69/12.98
Anomalous phasing power from inflection (acentric)	2.06
Figure of merit (centric/acentric)	0.82/0.82

Refinement

Resolution (Å)	20-2.0
Reflections	41592
Test reflections	4651
Number non-H atoms	4416
R_{work} (%)	0.1890
R_{free} (%)	0.2102
Average B factors ($Å^2$)	
protein	28.1
B_{12}	25.5
waters	38.5
cadmium/chlorine/PEG	38.8
rmsd bond length (Å)	0.0067
rmsd bond angles (^{o})	1.32
Ramachandran analysis	
most favored	90.7%
allowed	9.3%

[1]Numbers in parentheses refer to the highest resolution shell.

Table 1. Statistics of data collection, phasing and structure refinement.

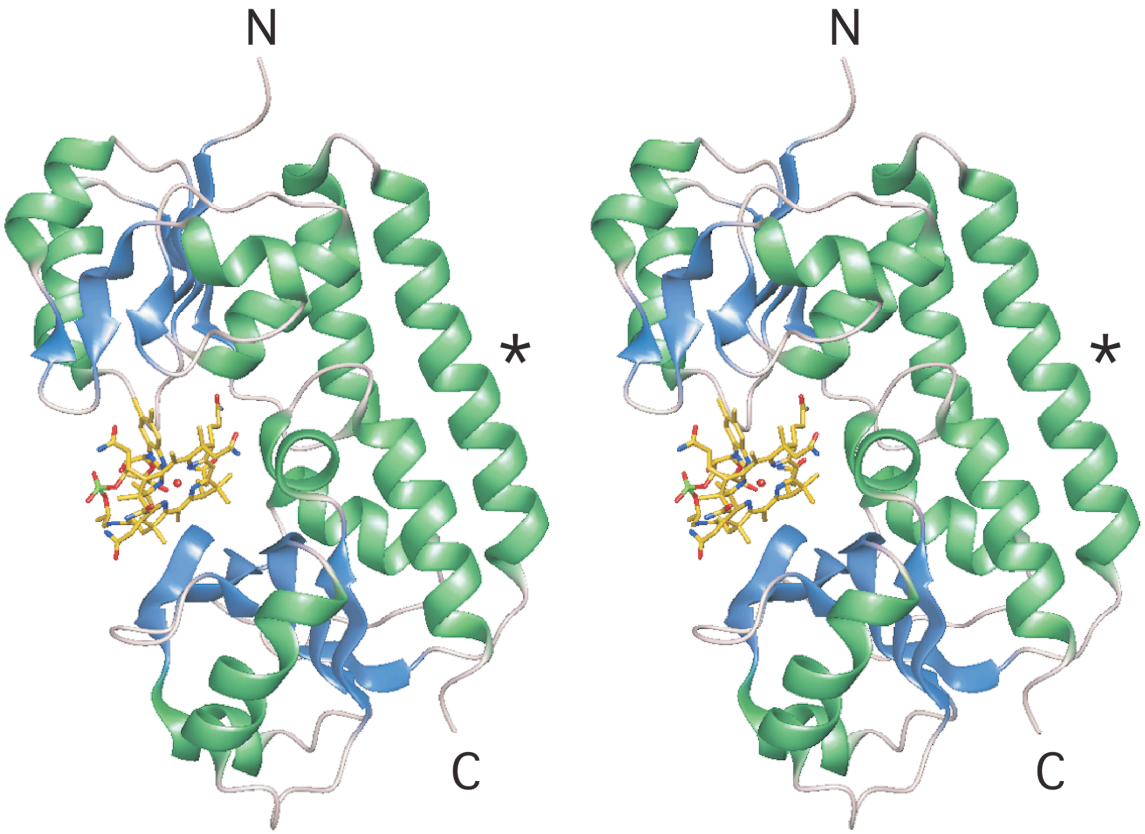

Figure 1. Structure of BtuF. A ribbon diagram of BtuF is shown in stereo with bound vitamin B_{12} in ball and stick. The N- and C-termini are labeled N and C, respectively. The backbone α-helix that bridges the two lobes of the protein is marked with an asterisk (see text).

A single, well-ordered molecule of vitamin B_{12} is bound in a deep cleft between the two lobes of BtuF (Fig. 1, 2). Similar to B_{12} free in solution, BtuF-bound B_{12} exists in the "base-on" conformation, i.e., with the N3B nitrogen of the dimethylbenzimidazole (DMB) base serving as an axial ligand to the central cobalt atom. A similar conformation of bound B_{12} has been observed in diol dehydratase (22) and class II ribonucleotide reductase (23). In contrast, B_{12} is bound in the base-off conformation by methionine synthase (24), methylmalonyl-coA mutase (25) and glutamate mutase (26). In these enzymes, the pseudo-nucleotide tail of B_{12} is extended and the nitrogen of a nearby

histidine side chain acts as an axial ligand to the cobalt. While B_{12} is bound by BtuF in the base-on conformation, it is not known if passage through the BtuCD transporter requires unfolding.

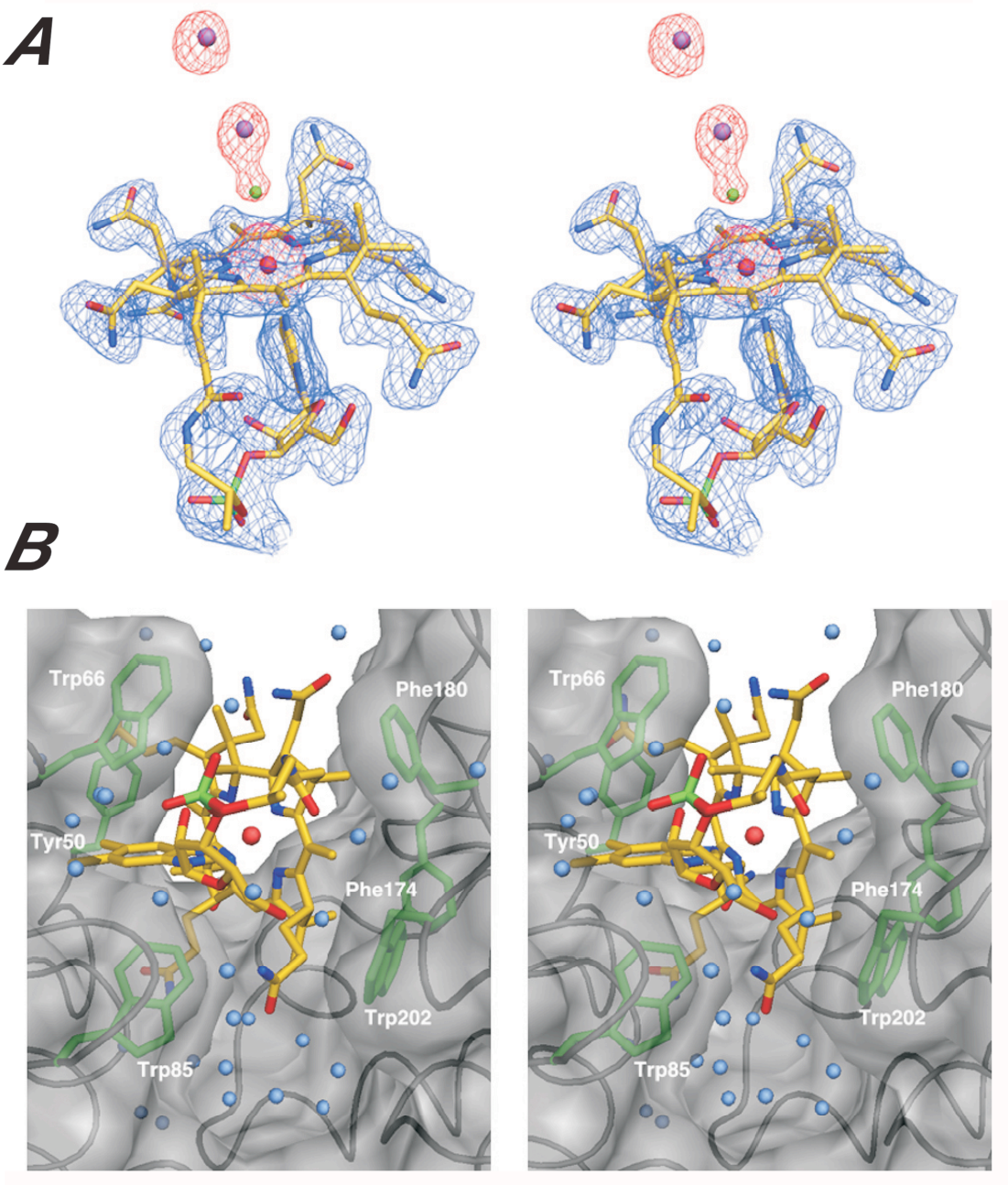

Figure 2. (previous page) Stereo view of vitamin B_{12} bound to BtuF. ***A***, B_{12} is shown in ball and stick with carbon atoms in yellow, oxygens in red, nitrogens in blue and phosphorus in green. The central cobalt atom is depicted as a red sphere. The experimental electron density at 2 Å resolution is shown as a blue mesh, contoured at 1.2 σ, while the anomalous difference Fourier density is shown as a red mesh and contoured at 8 σ. Cadmium and chlorine ions are shown as purple and green spheres, respectively. ***B***, B_{12} binding site. The BtuF backbone is shown in black and the molecular surface of BtuF in transparent gray. Side chains of six aromatic residues in van der Waals contact with B_{12} are colored green. B_{12} is shown as in ***A***, while water molecules are depicted as light blue spheres.

Six aromatic residues, three from each lobe of BtuF, contact B_{12} in the binding site (Fig. 2*B*). Two of these, Trp66 and Trp85, are situated on either side of the DMB group. In this respect, the binding site of BtuF resembles that of the ferrichrome binding protein FhuD (21). A network of ordered waters is observed between several corrin ring side chains and BtuF side and main chain atoms at the bottom of the binding site. There are also direct hydrogen bonds involving corrin ring side chains with the main chain nitrogen of Ala32 and the side chain atoms of Asp242 and Arg246. Although cyanocobalamin was used in the crystallization, no cyano group is apparent in the electron density at the upper axial ligand position. Instead, strong peaks in the anomalous difference Fourier map led us to model a chlorine ion (from the crystallization solution) with associated cadmium ions and water molecules (Fig. 2*A*). While these ions occupy this space in the crystal structure, there appears to be room for other axial ligands to the cobalt *in vivo*.

Conformational dynamics in BtuF structural homologs. The release of substrate into the translocation pathway of an ABC transporter is undoubtedly coupled to conformational changes in the binding protein (5). In the absence of transporter, binding

proteins such as the maltose binding protein (MBP) exhibit large hinge and twist movements of one lobe relative to the other between the liganded and unliganded states (7). In contrast, binding proteins such as BtuF and FhuD with a backbone α-helix are thought to be less likely to undergo such motions (19-21). Recently, the structure of one such binding protein, *T. pallidum* TroA, has been solved with (20) and without (27) bound Zn^{2+}. The difference between liganded and unliganded TroA was indeed found to be a mere 4° tilting of the C-terminal domain about the long axis of the protein without bending or unwinding of the backbone helix. This movement is very different from that observed for MBP and yet the result is a partial collapse of the binding site and the loss of the proper coordination geometry for Zn^{2+}.

A search using the Dali server (28) revealed that there is a striking structural similarity between the two lobes of BtuF and the αII and αIII domains of the molybdenum iron (MoFe) protein of nitrogenase (Z = 9.9 with 203 structurally equivalent residues) (29). Analogous to vitamin B_{12} in BtuF, the iron-molybdenum cofactor (FeMoco) is situated at the interface between the two domains. In the absence of cofactor (30), one of the two protein ligands to the FeMoco is shifted by ~5Å and other segments of the αIII domain are displaced or disordered, without a notable hinge movement or bending of the helix that corresponds to the backbone helix in BtuF. The differences in the structures of the cofactor-free MoFe protein compared to the MoFe holoprotein may be instructive for the potential conformational changes in binding proteins during the transport cycle, because, analogous to the rest of the MoFe protein, the membrane-spanning domains of the ABC transporter may constrain the movements of the two lobes of the attached binding protein.

BtuCD and BtuF interact *in vitro*. To show that the purified proteins used to determine the crystal structures can interact, BtuF and BtuCD were mixed at a molar ratio of approximately 5:1 (binding protein:transporter). A complex forms that is stable at 4° C for at least 72 hours and can be isolated by size exclusion chromatography. The presence of BtuF, BtuC and BtuD was confirmed by gel electrophoresis (Fig. 3) and the stoichiometry of the complex (1 BtuF : 2 BtuC : 2 BtuD) was determined by densitometry of the Coomassie stained gel.

A model for BtuF docking to BtuCD. The availability of the crystal structures of BtuF and BtuCD, combined with the evidence for their docking *in vitro*, provides an opportunity to model the interaction of an ABC transporter with its cognate binding

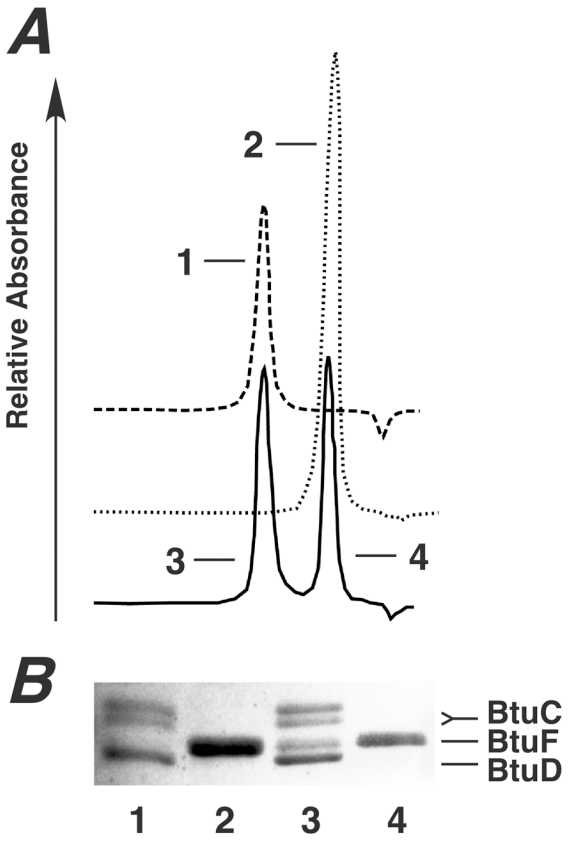

Figure 3. *In vitro* interaction of BtuF and BtuCD. ***A***, BtuF and BtuCD were mixed in detergent solution (0.1% LDAO) at a molar ratio of approximately 5:1 in the presence of vitamin B_{12}. The mixture was loaded onto an Superdex 200 10/30 column (Amersham Pharmacia) with pure BtuF (dotted line) and BtuCD (dashed line) as controls. Note that because of the presence of a large detergent micelle, pure BtuCD elutes at essentially the same volume as the complex of BtuCD and BtuF. ***B***, Peak fractions from the gel filtration chromatography shown in ***A*** were analyzed by SDS-PAGE. Lane numbers correspond to peaks as labeled in ***A***. Note that BtuC runs as a doublet.

protein. Electrostatic surface potential maps reveal two negatively charged "knobs" near the apex of each BtuF lobe and two positively charged "pockets" on the periplasmic surface of BtuC. The knobs on the surface of BtuF, corresponding to Glu72 and Glu202, are ~46 Å apart, with the vitamin B_{12} binding site located halfway between them. The pockets on BtuC are ~48 Å apart and are lined by three arginine residues: Arg56 and Arg59 from transmembrane helix TM2 and Arg295 from TM9. Both glutamates and all three arginines are conserved in iron siderophore/cobalamin transport systems from various organisms (Fig. 4*B* and *C*), suggesting that these residues may form inter-protein salt bridges that are critical for proper interaction of the binding protein with the transporter. When BtuF is manually docked onto the periplasmic face of BtuCD, aligning the conserved glutamates and arginines, bound B_{12} is positioned over the entrance to the translocation pathway (Fig. 4*A*).

A competitive peptide mapping study of FhuB, an ABC transporter for iron siderophores that is homologous to BtuCD, provides independent biochemical support for the proposed docking model of BtuF to BtuCD (31). It demonstrated that several peptides derived from FhuB bind to its cognate binding protein FhuD and inhibit transport of ferrichrome when introduced into the periplasm. One of these peptides corresponds to a

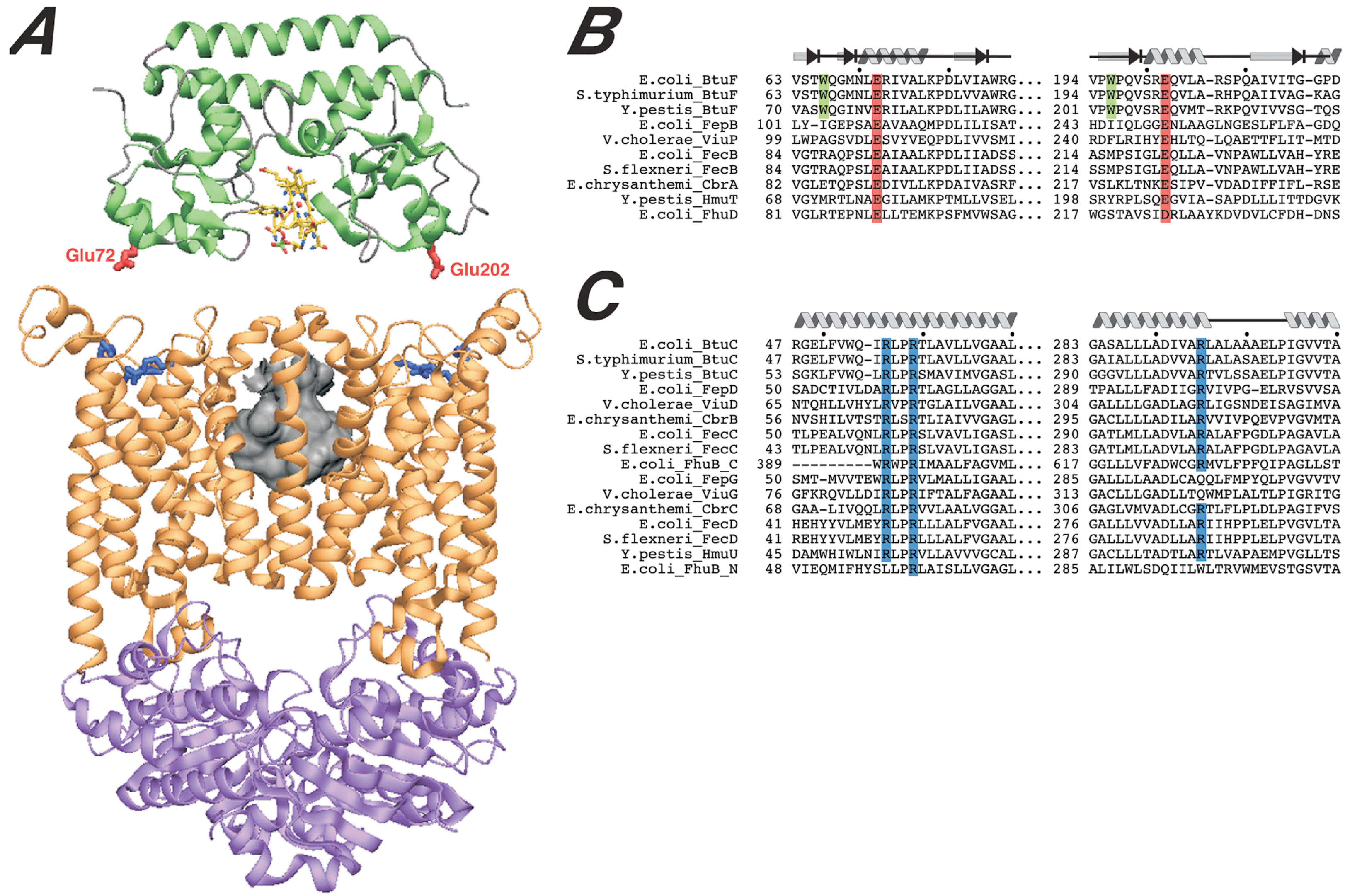
A
Glu72
Glu202
B
E.coli_BtuF 63 VSTWQGMNLERIVALKPDLVIAWRG... 194 VPWPQVSREQVLA-RSPQAIVITG-GPD
S.typhimurium_BtuF 63 VSTWQGMNLERIVALKPDLVVAWRG... 194 VPWPQVSREQVLA-RHPQAIIVAG-KAG
Y.pestis_BtuF 70 VASWQGINVERILALKPDLILAWRG... 201 VPWPQVSREQVMT-RKPQVIVVSG-TQS
E.coli_FepB 101 LY-IGEPSAEAVAAQMPDLILISAT... 243 HDIIQLGGENLAAGLNGESLFLFA-GDQ
V.cholerae_ViuP 99 LWPAGSVDLESVYVEQPDLIVVSMI... 240 RDFLRIHYEHLTQ-LQAETTFLIT-MTD
E.coli_FecB 84 VGTRAQPSLEAIAALKPDLIIADSS... 214 ASMPSIGLEQLLA-VNPAWLLVAH-YRE
S.flexneri_FecB 84 VGTRAQPSLEAIAALKPDLIIADSS... 214 SSMPSIGLEQLLA-VNPAWLLVAH-YRE
E.chrysanthemi_CbrA 82 VGLETQPSLEDIVLLKPDAIVASRF... 217 VSLKLTNKESIPV-VDADIFFIFL-RSE
Y.pestis_HmuT 68 VGYMRTLNAEGILAMKPTMLLVSEL... 198 SRYRPLSQEGVIA-SAPDLLLITTDGVK
E.coli_FhuD 81 VGLRTEPNLELLTEMKPSFMVWSAG... 217 WGSTAVSIDRLAAYKDVDVLCFDH-DNS
C
E.coli_BtuC 47 RGELFVWQ-IRLPRTLAVLLVGAAL... 283 GASALLLADIVARLALAAAELPIGVVTA
S.typhimurium_BtuC 47 RGELFVWQ-IRLPRTLAVLLVGAAL... 283 GAIALLLADVVARLALASAELPIGVVTA
Y.pestis_BtuC 53 SGKLFVWQ-LRLPRSMAVIMVGASL... 290 GGGVLLLADVVARTVLSSAELPIGVVTA
E.coli_FepD 50 SADCTIVLDARLPRTLAGLLAGGAL... 289 TPALLLFADIIGRVIVPG-ELRVSVVSA
V.cholerae_ViuD 65 NTQHLLVHYLRVPRTGLAILVGAAL... 304 GALLLLGADLAGRLIGSNDEISAGIMVA
E.chrysanthemi_CbrB 56 NVSHILVTSTRLSRTLIAIVVGAGL... 295 GACLLLLADILARVVIVPQEVPVGVMTA
E.coli_FecC 50 TLPEALVQNLRLPRSLVAVLIGASL... 290 GATLMLLADVLARALAFPGDLPAGAVLA
S.flexneri_FecC 43 TLPEALVQNLRLPRSLVAVLIGASL... 283 GATLMLLADVLARALAFPGDLPAGAVLA
E.coli_FhuB_C 389 ---------WRWPRIMAALFAGVML... 617 GGLLLVFADWCGRMVLFPFQIPAGLLST
E.coli_FepG 50 SMT-MVVTEWRLPRVLMALLIGAAL... 285 GALLLLAADLCAQQLFMPYQLPVGVVTV
V.cholerae_ViuG 76 GFKRQVLLDIRLPRIFTALFAGAAL... 313 GACLLLGADLLTQWMPLALTLPIGRITG
E.chrysanthemi_CbrC 68 GAA-LIVQQLRLPRVVLAALVGGAL... 306 GAGLVMVADLCGRTLFLPLDLPAGIFVS
E.coli_FecD 41 HEHYYVLMEYRLPRLLLALFVGAAL... 276 GALLLVVADLLARIIHPPLELPVGVLTA
S.flexneri_FecD 41 REHYYVLMEYRLPRLLLALFVGAAL... 276 GALLLVVADLLARIIHPPLELPVGVLTA
Y.pestis_HmuU 45 DAMWHIWLNIRLPRVLLAVVVGCAL... 287 GACLLLTADTLARTLVAPAEMPVGLLTS
E.coli_FhuB_N 48 VIEQMIFHYSLLPRLAISLLVGAGL... 285 ALILWLSDQIILWLTRVWMEVSTGSVTA

Figure 4. (previous page) Proposed interaction between BtuF and BtuCD. ***A***, BtuF and BtuCD are depicted as ribbon diagrams in an orientation that places the BtuF surface glutamates adjacent to conserved BtuC arginines (see text for further explanation). Once docked, the molecules were separated along the vertical axis for clarity. BtuF is shown in green, with the critical glutamates shown in ball and stick and colored red. BtuC and BtuD are shown in orange and purple respectively, with the critical BtuC arginines (Arg56, Arg59, Arg295) shown in ball and stick and colored blue. The size and location of the translocation pathway at the interface of the BtuC subunits (8) is represented by the molecular surface colored in gray. ***B***, Sequence alignment of iron siderophore/cobalamin binding proteins. The conserved surface glutamates are shown with a red background, with tryptophans contacting B_{12} on the green background. The secondary structure elements assigned for the *E. coli* BtuF structure are indicated above the sequence. ***C***, Alignment of the membrane-spanning subunits of the cognate ABC transporters with conserved arginines shown with a blue background. The secondary structure elements assigned for the structure of *E. coli* BtuC (8) are indicated above the sequence.

loop on the periplasmic surface of BtuC located between the conserved arginine pockets and the translocation pathway where it could interact with BtuF.

Despite significant differences in architecture, salt bridges may also play a crucial role for the interaction of the binding proteins for maltose and histidine, MBP and HisJ, with their cognate ABC transporters. When Glu214, located near the binding cleft of MBP, is mutated to lysine, maltose import is significantly impaired in an *in vivo* transport assay, even though binding of maltose to MBP appears unaffected (32). Similarly, mutations in HisJ at residues Asp144, Asp149 and Arg154 on lobe II of HisJ, have been shown to inhibit histidine transport with no significant effect on histidine binding (33). Mutation of Asp149 and Arg154 also inhibits ATP hydrolysis by the $HisQMP_2$ transporter. In addition, chemical cross-linking studies revealed that binding of these HisJ mutants to the membrane-spanning subunit of the transporter, HisQ, was impaired. While there is no high resolution structure of either the maltose or histidine transporter, these mutation

studies suggest that salt bridges between surface-exposed residues may play an important role in the attachment of binding proteins.

Conclusions

The structure of B_{12}-bound BtuF reveals that vitamin B_{12} is presented to the BtuCD transporter in the "base-on" conformation. Conserved acidic residues on the surface of BtuF may be important for interaction with BtuCD. Our observations provide a model for the docking of a periplasmic binding protein to its cognate ABC transporter. The ability to form a stable complex between BtuF and BtuCD should allow their docking to be studied structurally, which may reveal crucial conformational changes and provide a more detailed understanding of the B_{12} transport reaction.

References

1. Higgins, C. F. (2001) *Res. Microbiol.* **152,** 205-210.
2. Dean, M., Rzhetsky, A. & Allikmets, R. (2001) *Gen. Research* **11,** 1156-1166.
3. Nikaido, H. & Hall, J. A. (1998) *Methods Enzymol.* **292,** 3-20.
4. Boos, W. & Lucht, J. M. (1996) in *Escherichia coli and Salmonella typhimurium: Cellular and Molecular Biology*, ed. Neidhardt, F. C. (American Society for Microbiology, Washington, DC), Vol. 1, pp. 1175-1209.
5. Davidson, A. L. (2002) *J. Bacteriol.* **184,** 1225-1233.
6. Chen, J., Sharma, S., Quiocho, F. A. & Davidson, A. L. (2001) *Proc. Natl. Acad. Sci. USA* **98,** 1525-1530.
7. Quiocho, F. A. & Ledvina, P. (1996) *Mol. Microbiol.* **20,** 17-25.
8. Locher, K. P., Lee, A. T. & Rees, D. C. (2002) *Science* **296,** 1091-1098.
9. Van Bibber, M., Bradbeer, C., Clark, N. & Roth, J. R. (1999) *J. Bacteriol.* **181,** 5539-5541.
10. Cadieux, N., Bradbeer, C., Reeger-Schneider, E., Köster, W., Mohanty, A. K., Wiener, M. & Kadner, R. J. (2002) *J. Bacteriol.* **184,** 706-717.
11. Otwinowski, Z. & Minor, W. (1997) *Methods Enzymol.* **276,** 307-326.
12. Terwilliger, T. C. & Berendzen, J. (1999) *Acta Crystallogr.* **D55,** 849-861.
13. Fortelle, E. d. l. & Bricogne, G. (1997) *Methods Enzymol.* **276,** 472-494.
14. Collaborative Computational Project, N. (1994) *Acta Crystallogr.* **D50,** 760-763.
15. Jones, T. A., Zou, J.-Y., Cowan, S. W. & Kjeldgaard, M. (1991) *Acta Crystallogr.* **A47,** 110-119.

16. Brünger, A. T., Adams, P. D., Clore, G. M., DeLano, W. L., Gros, P., Grosse-Kunstleve, R. W., Jiang, J.-S., Kuszewski, J., Nilges, M., Pannu, N. S., Read, R. J., Rice, L. M., Simonson, T. & Warren, G. L. (1998) *Acta Crystallogr*. **D54,** 905-921.

17. Laskowski, R. A., MacArthur, M. W., Moss, D. S. & Thornton, J. M. (1993) *J. Appl. Cryst*. **26,** 283-291.

18. www.dino3d.org.

19. Lawrence, M. C., Pilling, P. A., Epa, V. C., Berry, A. M., Ogunniyi, A. D. & Paton, J. C. (1998) *Structure* **6,** 1553-1561.

20. Lee, Y.-H., Deka, R. K., Norgard, M. V., Radolf, J. D. & Hasemann, C. A. (1999) *Nature Struct. Biol*. **6**.

21. Clarke, T. E., Ku, S.-Y., Dougan, D. R., Vogel, H. J. & Tari, L. W. (2000) *Nature Struct. Biol*. **7,** 287-291.

22. Shibata, N., Masuda, J., Tobimatsu, T., Toraya, T., Suto, K., Morimoto, Y. & Yasuoka, N. (1999) *Structure* **7,** 997-1008.

23. Sintchak, M. D., Arjara, G., Kellogg, B. A., Stubbe, J. & Drennan, C. L. (2002) *Nature Struct. Biol*. **9,** 293-300.

24. Drennan, C. L., Huang, S., Drummond, J. T., Matthews, R. G. & Ludwig, M. L. (1994) *Science* **266,** 1669-1674.

25. Mancia, F., Keep, N. H., Nakagawa, A., Leadlay, P. F., McSweeney, S., Rasmussen, B., Bösecke, P., Diat, O. & Evans, P. R. (1996) *Structure* **4,** 339-350.

26. Reitzer, R., Gruber, K., Jogl, G., Wagner, U. G., Bothe, H., Buckel, W. & Kratky, C. (1999) *Structure* **7,** 891-902.

27. Lee, Y.-H., Dorwart, M. R., Hazlett, K. R. O., Deka, R. K., Norgard, M. V., Radolf, J. D. & Hasemann, C. A. (2002) *J. Bacteriology* **184,** 2300-2304.

28. www.ebi.ac.uk/dali.

29. Kim, J. & Rees, D. C. (1992) *Science* **257,** 1677-1682.

30. Schmid, B., Ribbe, M. W., Einsle, O., Yoshida, M., Thomas, L. M., Dean, D. R., Rees, D. C. & Burgess, B. K. (2002) *Science* **296,** 352-356.

31. Mademidis, A., Killmann, H., Kraas, W., Flechsler, I., Jung, G. & Braun, V. (1997) *Mol. Microbiol.* **26,** 1109-1123.

32. Szmelcman, S., Sassoon, N. & Hofnung, M. (1997) *Protein Science* **6,** 628-636.

33. Liu, C. E., Liu, P.-Q., Wolf, A., Lin, E. & Ames, G. F.-L. (1999) *J. Biol. Chem.* **274,** 739-747.